The 9th European Congress on Computational Methods in Applied Sciences and Engineering
ECCOMAS Congress 2024
3–7 June 2024, Lisboa, Portugal

ON THE NUMERICAL SIMULATION OF LEFT VENTRICLE BLOOD FLOW

ENEKO LAZPITA[1,*], MAHESH S. NAGARGOJE[1,3], ANDREA MARES[4], PEDRO QUINTERO[4], MICHAEL NEIDLIN[5], SOLEDAD LE CLAINCHE[1,2] AND JESÚS GARICANO-MENA[1,2]

[1] ETSI Aeronáutica y del Espacio, Universidad Politécnica de Madrid, Madrid, Spain
[2] Center for Computational Simulation (CCS), Boadilla del Monte, Spain
[3] LaBS-CompBiomech, Politecnico di Milano, Milan, Italy [4] Universitat Politècnica de València, Valencia, Spain [5] Aachen University, Aachen, Germany

[*] Corresponding author: e.lazpita@upm.es

Key words: Computational Fluid Dynamics, Cardiac Flow, Left Ventricle Model, Flow Patterns

Summary. Cardiovascular diseases remain a leading cause of morbidity and mortality globally, necessitating enhanced diagnostic and predictive methodologies. This study utilizes high-resolution computational fluid dynamics (CFD) tools to investigate the hemodynamics within the human left ventricle model, employing both Siemens StarCCM+ and Ansys Fluent for code comparison purposes. The simulations solve the incompressible Navier-Stokes equations, representing blood under physiologically realistic boundary conditions derived from a model cardiac geometry and dynamic ventricular wall motion. Mesh convergence tests confirm the reliability of the simulations, with refined meshing strategies ensuring numerical accuracy. Detailed analyses of flow features reveal the formation, progression, and interaction of vortex rings during the cardiac cycle, providing insights into the fluid mechanics that underpin efficient cardiac function.

1 INTRODUCTION

Cardiovascular diseases (CVDs) are the leading cause of mortality globally, responsible for an estimated 17.9 million deaths annually. This group of disorders, encompassing coronary artery diseases, cerebrovascular diseases, rheumatic heart diseases, and other conditions, not only leads to significant mortality but also contributes extensively to the burden of health care systems worldwide. Importantly, over 85% of these deaths are attributed to heart attacks and strokes, with a substantial portion occurring prematurely in individuals under 70 years of age.

The growing impact of CVDs create a necessity of evolving the diagnosis and treatments. In recent years, new perspectives has risen in medical research, offering new methodologies for understanding and treating complex diseases like CVDs. Among these, Computational Fluid Dynamics (CFD) has emerged as a pivotal tool in modeling the intricate dynamics of intracardiac blood flow. This approach not only aids in the fundamental understanding of heart function but also paves the way for innovative treatment strategies.

The work of Bucelli *et al.* [1] represents a significant milestone in the simulation of cardiac function that integrates multiple physical processes governing heart dynamics. Their model

innovatively couples cardiac electrophysiology, active and passive mechanics, and hemodynamics, incorporating reduced models for cardiac valves and the systemic circulation. Zingaro *et al.* [2] developed a computational model for simulating 3D blood flow in the left heart, integrating the Navier-Stokes equations with cardiac electromechanics and a systemic circulation model, validated by reproducing key hemodynamic indicators.

In this study, we focus on utilizing CFD to identify and characterize key vortical structures within the heart — such as vortex rings, recirculation zones, and swirls — which are critical to understanding the efficiency of blood pumping and are potentially indicative of various cardiac pathologies. Elbaz *et al.* [3] and Pedrizzetti *et al.* [4] provide compelling evidence that understanding these flow patterns can offer novel insights into left ventricular function and could serve as a predictive tool for early diagnosis and intervention in heart disease progression.

The objective of this paper is to review the existing methodology for conducting CFD to model heart dynamics. Specifically, this study aims to investigate the formation of vortices within the heart. To achieve this, we compare two well-established, `commercial` numerical solvers (Star-CCM+ and Fluent) and conduct a convergence study for both. The article seeks to clarify the appropriate methodology to follow when performing numerical simulations with an idealized heart geometry.

2 METHODOLOGY

To achieve a comprehensive analysis of the flow dynamics within the left ventricular chamber, this study incorporates Computational Fluid Dynamics (CFD) simulations conducted using two different `commercial` solvers: Star-CCM+ and Fluent. The use of multiple `commercial` solvers enables a comparative study of the simulation results, enhancing the reliability and accuracy of the study. Also for validation purposes, we are going to base our validation on the studies made by Zheng *et al.* [5] and Vedula *et al.* [6].

Therefore, the geometric configuration of the left ventricle (LV) model for our simulations is directly extracted from [5]. This model represents the LV model as a semi-ellipsoid, connected to cylindrical tubes which simulate the inflow and outflow ducts. For visual clarity and reference, a detailed schematic of this geometry is illustrated in Figure 1. The specific values for the parameters involved in the geometry are represented in Table 1. These dimensions are chosen to realistically approximate the geometrical proportions of the human LV model while facilitating detailed computational analysis. The tube lengths were fixed to 5 times the inlet diameter to ensure a good adaptation of the inflow when arriving to the ventricle.

Nomenclature	Description	Value [cm]
a	Short semiaxis	2
b	Long semiaxis	8
D	Inlet tube diameter	1.2
d	Outlet tube diameter	0.8
C	Distance to inlet tube center	0.55
c	Distance to outlet tube center	1.35
H	Tube lengths	5D

Table 1: Parameters that describe the geometrical features of the model.

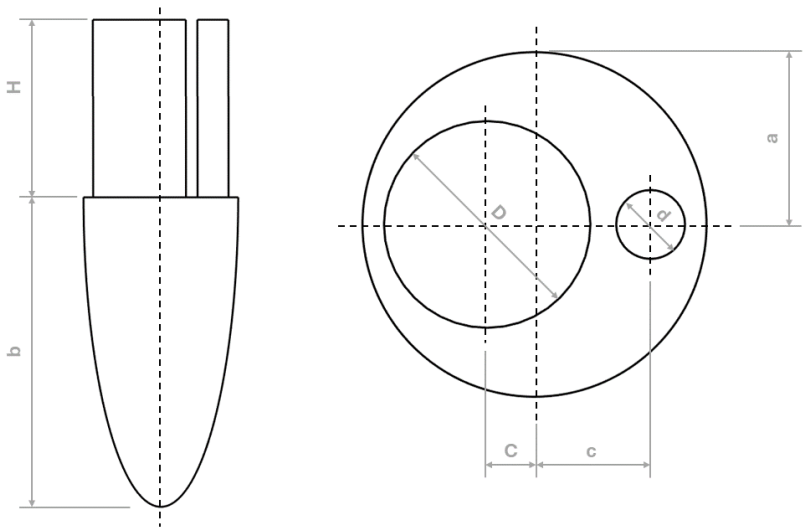

Figure 1: Ideal geometry of the LV model extracted from [5].

To simulate the dynamic changes in ventricular volume during the cardiac cycle, we refer to the flow rate data represented in Figure 2. From this graph we can extract the volume change of the ventricle through a strategy of integration and uniform expansion of the semi-ellipsoid. The end-systolic volume (ESV) is 67 ml and the end-diastolic volume (EDV) is 145 ml, leading to an estimated ejection fraction of approximately 0.54, calculated using the formula $EF = \frac{EDV-ESV}{EDV}$. This ejection fraction is critical for modeling the cardiac functions accurately and reflects realistic physiological conditions which should be between 0.5 and 0.7 values as explained in [7].

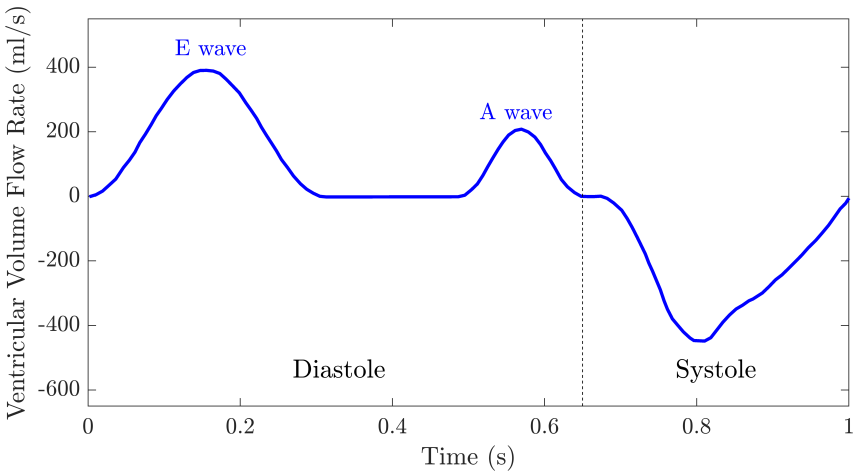

Figure 2: Ventricular volumetric flow rate chart extracted from [5].

3 SIMULATION SETUP

The computational framework employed in this study for both Star-CCM+ and Fluent is designed to solve the Navier-Stokes equations, and the most relevant setup selections are summarized in Table 2. We assume that the flow is incompressible, which is widely accepted in the simulation of human blood flow due to its high accuracy in such applications [8]. Building on prior research, we opt for modeling the blood flow as laminar. This choice is supported by evidence suggesting that laminar flow models are particularly effective in capturing the vortical features of the diastolic phase of the cardiac cycles [9, 10].

Boundary conditions are a critical aspect of any simulation setup. Inlet velocity profiles and outlet pressures or mass flow rates are defined, aligning with physiological norms to mirror actual cardiac conditions as closely as possible. For the Fluent implementation, we include some simulation run events that change the outlet boundary to wall for the diastole and the same for the inlet in systole to mimic the closing of the valves. The rest of the cycle are defined as velocity inlet or pressure outlet.

A particularly challenging aspect of simulating heart dynamics is the need for the ventricular walls to expand and contract dynamically with each cardiac cycle, while the inflow and outflow tubes remain static. To manage this, we implement a sophisticated meshing strategy that enhances resolution near the walls, crucial for capturing the boundary layer phenomena and maintaining numerical accuracy throughout the dynamic simulation [11]. The dynamic movement of the ventricle walls is crucial for replicating heart function. For this purpose, we utilize data from Figure 2 to calculate the volume changes at each time-step. The implementation of this aspect varies between the solvers. In Fluent, the distribution of the mesh points for each time instant must be pre-extracted and included as STL files during the simulation. In contrast, Star-CCM+ simplifies this process by requiring only the minimum and maximum volumes along with their transition evolution, utilizing its morphing feature to apply the necessary changes [12]. Both processes require maintaining the integrity and connectivity of the computational mesh as the geometry deforms to reduce the compromise of the mesh quality or simulation stability.

The outcome of this setup is depicted in Figure 3, which shows the ventricular cavity volume over time, mimicking realistic heart behavior. The simulation starts with a ventricular volume corresponding to the end-systolic volume (ESV) of 67 ml. The volume then increases during the E-wave and A-wave of diastole, reaching approximately 145 ml at $t/T \simeq 0.65$, the end-diastolic volume (EDV). Following this, the ventricle contracts during systole, expelling blood and returning to the initial ESV. This cycle repeats, providing a continuous, realistic representation of heart function across multiple cardiac cycles, crucial for validating our simulation approach and the effectiveness of our modeling strategy.

4 RESULTS

In this section, we present the results of our comparative study, which involves comparing simulations conducted using two industrial CFD solvers, Siemens StarCCM+ and Ansys Fluent. Our analysis aims to assess the accuracy and reliability of these simulations by comparing them with previous studies and established medical/physiological benchmarks. Before delving into the comparison, we first ensure that our simulations are well-posed and have converged adequately.

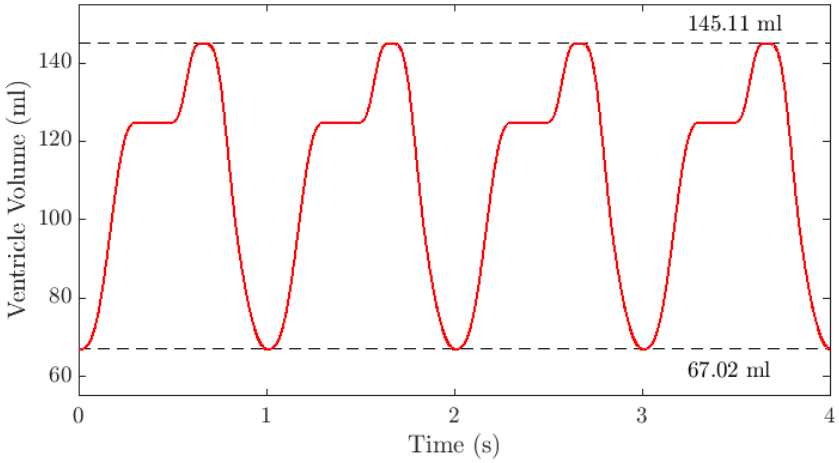

Figure 3: Evolution of LV model volume during four cycles of the heart.

`Commercial` solver	Ansys Fluent	Siemens Star-CCM+
Density (ρ)	1060 $kg/m^3 = cte$	
Viscosity (μ)	0.004 $Pa \cdot s = cte$	
Flow regime	Laminar	
Temporal discretization	2nd order	
Spatial discretization	2nd order	
Inlet	Velocity inlet, temporal profile	Velocity inlet (diastole), wall (systole)
Outlet	Mass flow outlet, temporal profile	Wall (diastole), pressure outlet (systole)
Wall movement	Morphing from ESV to EDV	UDF to introduce each time instant mesh

Table 2: Most relevant simulation setup for the different solvers.

4.1 Grid Convergence

To evaluate the convergence of our simulations with respect to mesh refinement, we employ four different mesh sizes, as detailed in Table 3. Our focus lies on examining the behavior of the total kinetic energy (TKE) within the LV model (excluding, of course, the inlet and outlet tubes) throughout the cardiac cycle.

Figure 4 illustrates the TKE distribution over time for both StarCCM+ and Fluent simulations, showcasing a consistent shape with slight variations in peak magnitudes. The overall curve shapes agree well with previous studies [6]. Additionally, as the mesh is refined, we observe a convergence towards a steady TKE distribution for each solver individually.

To further analyze convergence, we study the error between the different configurations and present the results in Table 3. We focus on two key indices: the convergence ratio (R) and the relative error. The convergence ratio R quantifies the convergence behavior between different mesh configurations, ensuring that $0 < R < 1$ for all cases. Meanwhile, the relative error estimates the difference between grid solutions, providing insights into the accuracy of the simulation results.

$$R = \frac{f_j - f_{j+1}}{f_{j+1} - f_{j+2}}, \text{ and} \tag{1}$$

$$\text{Relative error} = \left| \frac{f_j - f_{j+1}}{f_j} \right| \cdot 100, \tag{2}$$

where f_j in our case would be the TKE distribution in the fine mesh, while f_{j+1} and f_{j+2} would be the TKE in coarser meshes.

For both StarCCM+ and Fluent, the convergence ratio meets the specified criterion across various configurations. Notably, the relative error values for the medium-sized meshes in both `commercial` solvers are low, suggesting adequate convergence. Therefore, subsequent results presented in this section have been obtained using these mesh configurations, ensuring reliable and consistent outcomes.

Mesh size	Siemens StarCCM+		Ansys Fluent	
	Nº elem.	Relative error	Nº elem.	Relative error
Very coarse	0.3	7.82	0.3	13.62
Coarse	0.6	2.06	0.8	5.59
Medium	0.9	0.42	2.0	1.72
Fine	1.2	-	2.5	-

Table 3: The number of elements and the relative error for each solver and mesh employed.

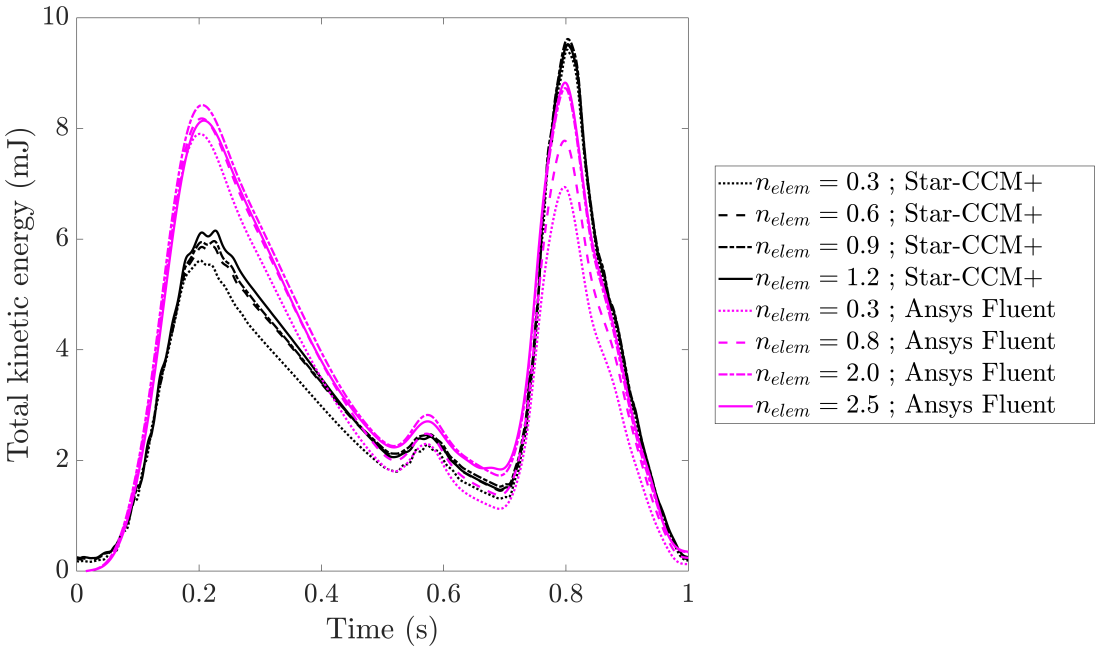

Figure 4: Evolution of the total kinetic energy for a heart cycle, for the different mesh sizes considered.

4.2 Flow Characteristics

As noted in the introduction, there is increasing evidence that changes in cardiac flow dynamics often precede detectable physiological alterations, providing the opportunity for early detection and intervention in cardiac disease. Accordingly, there is a growing interest in understanding the flow patterns and structures within the heart, particularly in the LV model, as this knowledge holds promise for the preventive detection and treatment of disease.

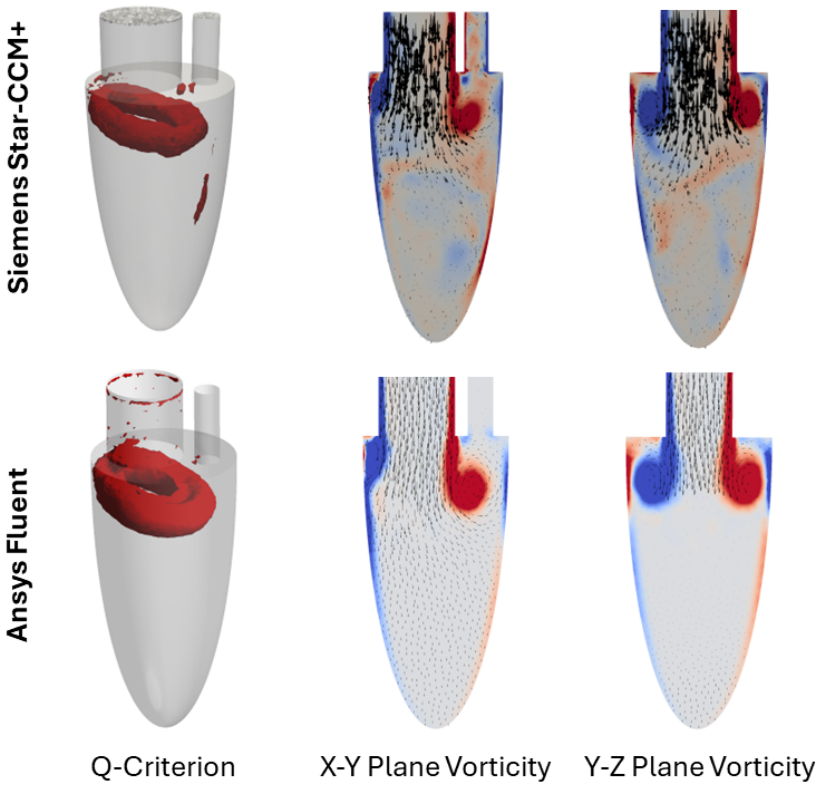

Figure 5: Comparison of the vortex ring formation at $t = 0.16s$ for Star-CCM+ in the top row and Fluent in the bottom row. Isocontours of the Q-Criterion (left) and the contours of the in-plane normal vorticity together with the velocity vectors for the X-Y plane (center) and the Y-Z plane (right).

In this section, we delve into the analysis of the most relevant flow feature observed in the ventricular flow throughout the cardiac cycle, the vortex ring. It is a prominent flow feature during the E-wave of diastole, as it plays a crucial role in cardiac hemodynamics and has been studied extensively in the literature [13, 14]. We mainly focus on examining its formation.
During the initial phase of diastole, the flow of blood begins to enter the left ventricle at an increasing velocity, as illustrated in Fig. 2. This is depicted in the early part of the heart cycle, where the flow rate is observed to increase. At this stage, the vortex ring emerges from the mitral valve with its axis aligned with the mitral valve axis. At this stage, the ring exhibits a circular shape but is asymmetric, with a thinner profile in proximity to the wall, which is indicative of a healthy heart. Subsequently, the ring travels through the ventricle, tilting due to the presence of the wall, and ultimately dissipates.

Figure 5 depicts the formation of the vortex ring at $t = 0.16s$, comparing the performance of both commercial solvers, Star-CCM+ and Fluent, as the top and bottom rows, respectively. First, in the left column, we present the isocontours of the Q-criterion within the LV model, which demonstrate that the vortex ring is aligned with the mitral valve axis and exhibits a thinner profile in proximity to the wall for both solvers. Moreover, the impact of the vortex ring is discernible in the vorticity and velocity fields within the ventricle. In the center and right columns of the Fig. 5, we plot these fields in two different planes that cut through the model. The first is the symmetry plane of the model, and the second is a Y-Z plane that cuts through the center of the inlet tube. In the symmetry plane, which is located in the center column of the image, the asymmetric formation of the vortex ring is more clearly discernible, with the size of the swirl closer to the wall being smaller. Moreover, the influence of the wall is evident in the tilting of the ring at this stage, as evidenced by the red swirl traveling deeper into the ventricle. In the right column, where the Y-Z plane normal vorticity is depicted, the alignment of the vortex ring axis and the mitral valve, as well as the symmetric nature of the vortical features in the Z direction, are clearly discernible.
Notably, while the TKE plots did not completely overlap between the solvers, both solvers demonstrated remarkable consistency in capturing the flow characteristics and the formation and evolution of the vortex ring. This agreement extends not only between the two solvers but also aligns closely with findings documented in the existing literature [5, 6].

5 Conclusion

This study has employed advanced CFD simulations using both Siemens StarCCM+ and Ansys Fluent to investigate the hemodynamics within a LV model. By leveraging these simulations, we aimed to cross-validate findings against known physiological behaviors and prior computational studies to ensure the robustness and reliability of our results.

Our mesh convergence tests indicated that with refined meshing strategies, both simulation platforms achieved grid converged results that were consistent with each other and aligned with established data, as detailed in the literature. From the TKE graph we can also see that even though the peak values have differences, the shape and distribution in time matches between Ansys Fluent and Siemens Star-CCM+.

Moreover, both simulations provided a detailed and similar view of how the vortex ring develops during the E-wave of diastole, a critical phase for efficient blood filling in the LV model. These observations were not only consistent between both our solvers but with previous studies too, which enforces our validation of the simulations and the conditions selected.

In conclusion, this study underscores the efficacy of using multiple CFD tools to gain insights into the complex fluid dynamics of the heart. Future research could expand upon this foundation by exploring patient-specific geometries and including pathological conditions, and aid in the design of more effective treatments and interventions for heart disease. The combination of StarCCM+ and Fluent provides a robust platform for such exploratory and diagnostic endeavors in cardiac health.

ACKNOWLEDGEMENTS

The authors acknowledge the grants PID2020-114173RB-I00, TED2021- 129774B-C21 and PLEC2022-009235 funded by MCIN/AEI/ 10.13039/501100011033 and by the European Union

"NextGenerationEU"/PRTR, and S.L.C. acknowledges the support of Comunidad de Madrid through the call Research Grants for Young Investigators from Universidad Politécnica de Madrid. The authors gratefully acknowledge the Universidad Politécnica de Madrid (www.upm.es) for providing computing resources on Magerit Supercomputer.

REFERENCES

[1] Bucelli, M., Zingaro, A., Africa, P.C., Fumagalli, I., Dede', L. and Quarteroni, A., 2023. "A mathematical model that integrates cardiac electrophysiology, mechanics, and fluid dynamics: Application to the human left heart." Int. J. Numer. Method. Biomed. Eng., 39(3), p.e3678. https://doi.org/10.1002/cnm.3678

[2] Zingaro, A., Fumagalli, I., Dede, L., Fedele, M., Africa, P.C., Corno, A.F. and Quarteroni, A., 2022. "A multiscale CFD model of blood flow in the human left heart coupled with a lumped-parameter model of the cardiovascular system." Discr. Cont. Dynam. Syst., 15, pp.2391-427.

[3] Elbaz, M.S., Calkoen, E.E., Westenberg, J.J., Lelieveldt, B.P., Roest, A.A. and Van Der Geest, R.J., 2014. "Vortex flow during early and late left ventricular filling in normal subjects: quantitative characterization using retrospectively-gated 4D flow cardiovascular magnetic resonance and three-dimensional vortex core analysis." J. Cardiovasc. Magn. Reson., 16(1), p.78. https://doi.org/10.1186/s12968-014-0078-9

[4] Pedrizzetti, G., La Canna, G., Alfieri, O. and Tonti, G., 2014. "The vortex—an early predictor of cardiovascular outcome?". Nat. Rev. Cardiol., 11(9), pp.545-553. https://doi.org/10.1038/nrcardio.2014.75

[5] Zheng, X., Seo, J.H., Vedula, V., Abraham, T. and Mittal, R., 2012. "Computational modeling and analysis of intracardiac flows in simple models of the left ventricle." Eur. J. Mech. B Fluids, 35, pp.31-39. https://doi.org/10.1016/j.euromechflu.2012.03.002

[6] Vedula, V., Fortini, S., Seo, J.H., Querzoli, G. and Mittal, R., 2014. "Computational modeling and validation of intraventricular flow in a simple model of the left ventricle." Theor. Comput. Fluid Dyn., 28, pp.589-604. https://doi.org/10.1007/s00162-014-0335-4

[7] Sawyer, D.B. and Vasan, R.S., 2017. "Encyclopedia of cardiovascular research and medicine." Elsevier.

[8] Morris, P.D., Narracott, A., von Tengg-Kobligk, H., Soto, D.A.S., Hsiao, S., Lungu, A., Evans, P., Bressloff, N.W., Lawford, P.V., Hose, D.R. and Gunn, J.P., 2016. "Computational fluid dynamics modelling in cardiovascular medicine." Heart, 102(1), pp.18-28.

[9] He, G., Han, L., Zhang, J., Shah, A., Kaczorowski, D.J., Griffith, B.P. and Wu, Z., 2022. "Numerical study of the effect of LVAD inflow cannula positioning on thrombosis risk." Comput. Methods. Biomech. Biomed. Engin., 25(8), pp.852-860. https://doi.org/10.1080/10255842.2021.1984433

[10] Colorado-Cervantes, J.I., Nardinocchi, P., Piras, P., Sansalone, V., Teresi, L., Torromeo, C. and Puddu, P.E., 2022. "Patient-specific modeling of left ventricle mechanics." Acta Mechanica Sinica, 38(1), p.621211. https://doi.org/10.1007/s10409-021-09041-0

[11] Moreno, R., Nicoud, F., Veunac, L. and Rousseau, H., 2006. "Non linear transformation field to build moving meshes for patient specific blood flow simulations." ECCOMAS Conference.

[12] Xu, F. and Kenjereš, S., 2021. "Numerical simulations of flow patterns in the human left ventricle model with a novel dynamic mesh morphing approach based on radial basis function." Comput. Biol. Med., 130, p.104184. https://doi.org/10.1016/j.compbiomed.2020.104184

[13] Le, T.B., Sotiropoulos, F., Coffey, D. and Keefe, D., 2012. "Vortex formation and instability in the left ventricle." Phys. Fluids, 24(9).

[14] Le, T.B., Elbaz, M.S., Van Der Geest, R.J. and Sotiropoulos, F., 2019. "High resolution simulation of diastolic left ventricular hemodynamics guided by four-dimensional flow magnetic resonance imaging data." Flow, Turbulence and Combustion, 102, pp.3-26.